# Sensor selection for state estimators based on the estimation performance of predefined quantities of interest

**T. Devos** [1,2], **L. Kennes** [1], **M. Viehweger** [1,2], **M. Kirchner** [1,2], **J. Croes** [1,2], **F. Naets** [1,2]
[1] KU Leuven, Department of Mechanical Engineering,
Celestijnenlaan 300, B-3001, Heverlee, Belgium

[2] DMMS Core Lab, Flanders Make, Belgium
e-mail: **thijs.devos@kuleuven.be**

## Abstract
Since more complex, system-level models typically have more states, estimators featuring such models are prone to experiencing more issues towards observability during operation. This leads to a larger minimal sensor set required for full observability although many of these sensors do not contribute sufficiently to the estimation performance of the quantities of interest. Additionally, sensor selection is often done by trial-and-error while most model or data-based algorithms only work for a few specific types of sensors. This work applies a novel sensor selection methodology presented in previous work capable of handling partially unobservable systems by applying an observable transformation. This is done by saving the linearized Jacobians determined using an EKF-based estimation framework to rank the sensors according to their contribution to the estimation performance of the estimator quantities of interest. The methodology has been validated for a vehicle case prior to acquiring sensors to show the potential of the methology.

## 1 Introduction

Over the past decades, there is a general trend towards smart and energy efficient systems due to stricter requirements towards user safety, comfort and emissions. Because mechatronic systems tend to become more complex, more information is required to accurately control their subsystems in order to ensure safe and environment friendly operation. For direct information acquisition, sensors are installed capable of directly measuring these quantities. However, some relevant information is often either not directly measurable or very hard to measure either because the sensors are simply not available on the market, or the available sensors are very expensive or intrusive. This has lead to the development of advanced estimation algorithms as they can provide a cost-effective alternative to obtain relevant operational system information. Therefore, these estimation algorithms have gained significant traction over the past years in research.

An important part of the development of an estimator is sensor selection as this has an immediate effect on the estimation accuracy. This is commonly done using trial-and-error because sensors typically have to be acquired before their performance can be assessed. However, this is very costly and time intensive and does not guarantee the best sensor set is chosen. Therefore, it would be much more cost-efficient to acquire insight on the estimation performance of different sensors before they have to be bought. To achieve this, several approaches to solve this issue have been investigated in previous research varying from model-based approaches [1] to machine learning methodologies [2].

Due to the rise in system complexity, more complex models are required which capture sufficient physics. Because more complex models typically feature more states, this poses additional challenges with respect to observability as all states need to be observable for stable operation. Additionally, the more model states, the more sensors are required to make the estimator fully observable although many of these sensors might not

sufficiently contribute to the estimation performance. As a results, there is a minimally required amount of sensors needed for full observability which increases with model complexity. Previous research has shown that it is possible to stabilize unobservable state covariance given their independence to the quantities of interest using an observable projection [3]. This allows fewer sensors to be needed for stable estimator operation compared to the required amount for full observability. In this work, the sensor selection methodology presented in [3] is explained and applied to a complex vehicle model to investigate the estimation performance of certain sensors and to determine which states are not relevant in the dynamic model.

In section 2, the general estimation framework is presented. The section presents the equations of motion, measurements and quantities of interest as well as equations required for observability analysis and dynamic coupling analysis. Section 3 explains the application of the sensor selection methodology presented in [3] which starts with measurement generation in subsection 3.1, continues with a forward simulation using the Extended Kalman Filter (EKF) where all relevant information is saved such as the linearized Jacobians. Subsequently, the sensor selection algorithm is evaluated which ranks the sensors according to their relative contribution to the estimation performance of the quantities of interest, expressed by their covariances. Section 4 presents the validation of the methodology on a vehicle case and finally section 5 summarizes the conclusions.

## 2 General Estimation Framework

The sensor selection methodology presented in this paper uses a general estimator framework from literature presented in [3] and is built upon three main equations namely the system, measurements and quantities of interest equations. To keep the framework as generally applicable as possible, non-linear equations are used and can be expressed as:

$$\text{System:} \qquad \dot{\mathbf{x}} = \mathbf{f}(\mathbf{x}, \mathbf{u}, t) \tag{1}$$

$$\text{Measurements:} \qquad \mathbf{y} = \mathbf{h}(\mathbf{x}, \mathbf{u}, t) \tag{2}$$

$$\text{Quantities of Interest:} \qquad \mathbf{y}_{vs} = \mathbf{g}(\mathbf{x}, \mathbf{u}, t) \tag{3}$$

where $\mathbf{u}$ are the inputs, $\mathbf{x}$ represents the state vector and $\dot{\mathbf{x}}$ describes its time derivative. The vectors $\mathbf{y}$ and $\mathbf{y}_{vs}$ quantify respectively the measurements and quantities of interest and $t$ is the time.

The objective of the estimator is to reliably estimate the quantities of interest or virtual sensors (VS), expressed by eq. (3). Therefore, the sensor selection algorithm presented in this work focuses on maximizing the estimation performance of these quantities of interest. To start off, the non-linear equations of motion need to be linearized, discretized and integrated. Subsequently, an observability analysis is performed together with dynamic coupling analysis to evaluate which sensors are required for full observability.

### 2.1 Linearization, Discretization and Integration

In this work, an Extended Kalman Filter (EKF) is applied to synchronize the model with the dynamics of the real vehicle [4]. As this filter requires a discrete time, linearized state-space formulation, the non-linear equations defined above are linearized and discretized. Linearization is performed using the central differencing scheme which is defined below for the continuous-time system Jacobian [5]:

$$\mathbf{F}_{c,k} = \frac{\partial \mathbf{f}(\mathbf{x}, \mathbf{u}, t)}{\partial \mathbf{x}}\Big|_{\mathbf{x}_k, \mathbf{u}_k, t_k} \approx \frac{\mathbf{f}(\mathbf{x}_k + \epsilon/2, \mathbf{u}_k, t_k) - \mathbf{f}(\mathbf{x}_k - \epsilon/2, \mathbf{u}_k, t_k)}{\epsilon} \tag{4}$$

where $\epsilon$ is a small perturbation factor. Similarly to the system Jacobian, the measurement and quantities of interest Jacobians $\mathbf{B}_k$, $\mathbf{H}_k$, $\mathbf{D}_k$, $\mathbf{G}_k$ and $\mathbf{E}_k$ are calculated. The central difference scheme tends to deliver more accurate results than both the forward and backward scheme although being more computationally demanding.

Furthermore, the continuous system Jacobian $\mathbf{F}_{c,k}$ is discretized to obtain the required discrete-time system Jacobian $\mathbf{F}_{d,k}$. In this work, the exponential discretization scheme has been used defined as [6]:

$$\mathbf{F}_{d,k} = e^{\mathbf{F}_{c,k}\Delta t} \tag{5}$$

where $\Delta t$ is the sampling time of the estimator. These linearized Jacobians are the basic requirement for the evaluation of the proposed sensor selection algorithm as they are needed in the estimator covariance equations. Acquiring them can be done by running the estimator for a specified virtual trajectory and saving the required Jacobians for every timestep or by exporting them from commercial software during a simulation.

Finally, the model equations can be rewritten into discrete state-space format where model integration is done using the previously calculated linearized and discretized Jacobians $\mathbf{F}_{d,k}$ and $\mathbf{B}_k$:

$$\mathbf{x}_{k+1} = \mathbf{F}_{d,k}\mathbf{x}_k + \mathbf{B}_k\mathbf{u}_{k+1} \tag{6}$$

$$\mathbf{y}_{k+1} = \mathbf{H}_k\mathbf{x}_{k+1} + \mathbf{D}_k\mathbf{u}_{k+1} \tag{7}$$

$$\mathbf{y}_{vs,k+1} = \mathbf{G}_k\mathbf{x}_{k+1} + \mathbf{E}_k\mathbf{u}_{k+1} \tag{8}$$

where $\mathbf{F}_{d,k}$, $\mathbf{H}_k$ and $\mathbf{G}_k$ represent the Jacobians with respect to the states and $\mathbf{B}_k$, $\mathbf{D}_k$ and $\mathbf{E}_k$ the Jacobians with respect to the inputs.

Due to the inherent nature of the main estimator equations defined in eq. (1) to eq. (3), sensors required for observability do not necessarily have a large impact on the estimation performance of the quantities of interest. This will depend on the coupling of the sensor equations to the internal model states which are required to evaluate the quantities of interest. To acquire a better overview of which sensors are required for a fully observable estimator, an extensive observability analysis is performed together with a dynamic coupling analysis.

## 2.2 Observability and Dynamic Coupling Analysis

In this work, observability analysis is performed based on the Kalman observability matrix as described for linear, time-invariant systems in [4]. However, for non-linear system and measurement equations, a distinction has to be made between local and global observability [7]. Therefore, to evaluate local observability, the Kalman observability matrix can be calculated at a specific timestep $k$ as:

$$\boldsymbol{\mathcal{O}}_k = \begin{bmatrix} \mathbf{H}_k \\ \mathbf{H}_k\mathbf{F}_{d,k} \\ \mathbf{H}_k\mathbf{F}_{d,k}^2 \\ \vdots \\ \mathbf{H}_k\mathbf{F}_{d,k}^{n-1} \end{bmatrix} \tag{9}$$

where $\mathbf{H}_k$ is the linearized measurement Jacobian, $\mathbf{F}_{d,k}$ is the linearized, discrete system Jacobian and $n$ is the amount of model states. These matrices can be calculated for every timestep at which linearization is executed. Fortunately, as the proposed sensor selection algorithm requires a predefined (virtual) trajectory, global observability can be easily investigated. In this work, global observability is evaluated using the total observability matrix as defined in [3] and reads:

$$\boldsymbol{\mathcal{O}}_{tot} = \begin{bmatrix} \boldsymbol{\mathcal{O}}_{k=1} \\ \boldsymbol{\mathcal{O}}_{k=1+p} \\ \boldsymbol{\mathcal{O}}_{k=1+2p} \\ \vdots \\ \boldsymbol{\mathcal{O}}_{k=m} \end{bmatrix} \tag{10}$$

where the subscript $p$ is an integer larger than 1 which indicates the level of global observability is taken into account and $m$ determines the total amount of matrices taken into account. The higher $p$, the more accurate global observability is evaluated but also the larger $\boldsymbol{\mathcal{O}}_{tot}$ will be as more timesteps are taken into account.

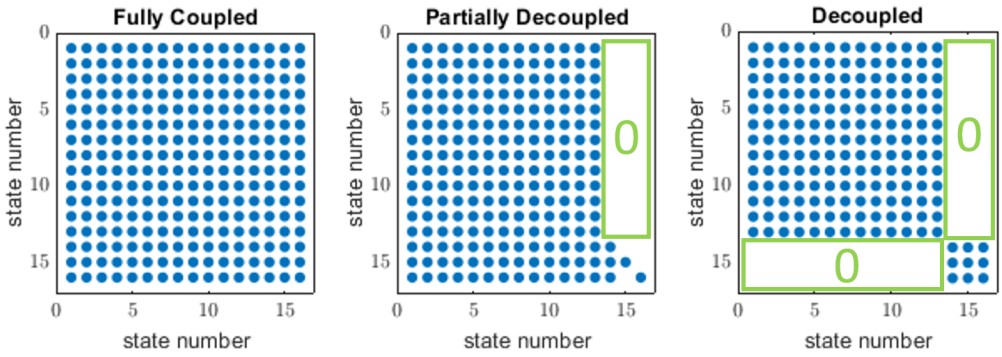


Figure 1: Fully coupled versus partially decoupled versus completely decoupled states as defined in [9].

Using eq. (10), the estimator can be defined as globally observable if the rank of the total observability matrix is equal to the amount of model states. The rank of a matrix can be calculated by considering a Singular Value Decomposition (SVD) of the respective matrix [8]:

$$\boldsymbol{\mathcal{O}}_{tot} = \mathbf{U}\boldsymbol{\Sigma}\mathbf{V} \tag{11}$$

where $\boldsymbol{\Sigma}$ represents the singular value matrix and $\mathbf{V}$ the corresponding singular modes. When one (or more) singular value(s) reach close to zero, this indicates that one (or more) state(s) are unobservable. If the unobservable states are independent of the quantities of interest, it is possible to stabilize the estimator covariance equations by transforming the states as [3]:

$$\mathbf{x} = \mathbf{V}_o^T \mathbf{q} \tag{12}$$

where $\mathbf{V}_o$ represents an observable projection matrix and $\mathbf{q}$ represent the corresponding modal contributions. This transformation matrix $\mathbf{V}_o$ can be acquired in various ways:

- Deduced from the Singular Modeset $\mathbf{V}$ where the modes corresponding to non-zero singular values are used
- A part of the unity matrix deliberately chosen to eliminate unobservable modes in the covariance update equations

Using the transformation defined in eq. (12), new Jacobians can be found which lead to transformed estimator equations. The detailed equations can be found in [3] and will not be repeated here.

It is important to note that the aforementioned transformation only works if the unobservable states are independent of the quantities of interest. This can be investigated at every timestep by evaluating the following equation:

$$\mathbf{G}_k \mathbf{V}_u^T = \mathbf{0} \tag{13}$$

where $\mathbf{V}_u$ is the kernel of the total observability matrix. Eq. (13) states that the quantities of interest Jacobian $\mathbf{G}_k$ cannot be part of the kernel of the total observability matrix. In other words, the quantities of interest cannot depend on the unobservable system states. If this is the case, sensors have to be added to make all relevant states observable.

The above defined transformation is important as it can stabilize the estimator implementation for unobservable systems. This makes it possible to eliminate more sensors than theoretically required for full observability, given their independence towards the quantities of interest. This poses interesting challenges towards sensor selection algorithms as extra information on observability can be taken into account. The sensor selection methodology used in this work is able to rank the sensors by their respective estimation performance contribution while preserving estimator stability.

To investigate which sensors are required to obtain a fully observable estimator, dynamic coupling analysis can be applied [3]. This is done by analysing the coupling between model states based on the linearized, discrete system Jacobian $\mathbf{F}_{d,k}$ evaluated at any timestep $k$. Depending on the contributions within the Jacobian,

three main cases can be defined according to figure 1. Although for simple systems, the conclusions from this analysis are rather straightforward, this does not necessary hold for large systems with lots of states. For large amount of states, it is possible to see a mixture of the three cases presented in figure 1. This is further explained on the vehicle case in section 4.

# 3 Sensor Selection Methodology

Using the estimator framework defined in section 2, the sensor selection methodology will be presented in this section. The methodology is based on previous work presented in [3] and requires the linearized Jacobians to be known for an entire simulation. For validation in this work, the assumption was made that no prior sensor data was available which could enable a trial-and-error estimator design based on the available data.

Therefore, the first step is to acquire the linearized Jacobians by running the estimator for predefined inputs. In order to be able to run the estimator, measurement data needs to be generated. Furthermore, the estimator is executed once to obtain and save the linearized Jacobians. Finally, the EKF covariance equations are consecutively executed to determine the sensor performance and rank them. These processes are described in the following subsections.

## 3.1 Measurement Data Generation

The generation of measurement data can be done in two ways namely either by using real measurements or generating virtual measurements:

**Virtual** Measurements are generated by performing a forward simulation and subsequently adding white noise to the simulation outputs $\mathbf{y}$ calculated using eq. (7). This approach can be used if measurement data is unavailable:

$$\mathbf{y}_m = \mathbf{y} + \boldsymbol{\mathcal{N}}(0, \boldsymbol{\sigma}) \tag{14}$$

**Real** Measurements generated from physical sensors logged during a test campaign.

Real measurements have the advantage that they represent a physical operating condition of the system but at the same time requires the acquisition of sensors and a costly test campaign which is often not desirable. Therefore, virtual measurement can also be considered which are obtained from a forward simulation using eqs. (6) to (8) for which no sensors have to be acquired. In this work, virtual measurements are generated through a forward simulation and adding white noise.

## 3.2 Estimator Simulation

After measurement data has been generated, the estimator is executed once to evaluate all linearized Jacobians which will later be used for evaluation during the sensor selection methodology. This is done by evaluating eqs. (4) to (8) for the entire sensor space such that all sensor equations are present in the measurement Jacobian $\mathbf{H}_k$. During this simulation, all Jacobians are saved for every timestep. Furthermore, the reference covariance $p_0$ used in the sensor selection methodology is obtained since the entire sensor space is taken into account during this simulation. After both the measurements are available and the linearized Jacobians, the sensor selection ranking procedure can be evaluated which is discussed in the next section.

## 3.3 Sensor Selection Algorithm

When the linearized Jacobians $\mathbf{F}_{d,k}$, $\mathbf{H}_k$ and $\mathbf{G}_k$ have been calculated for all timesteps $k$, the sensor selection algorithm can be evaluated. The methodology used has been visualized on figure 2 and is based on previous methods presented in [3]. The methodology can be executed for each quantity of interest and consists of 3 consecutive steps:

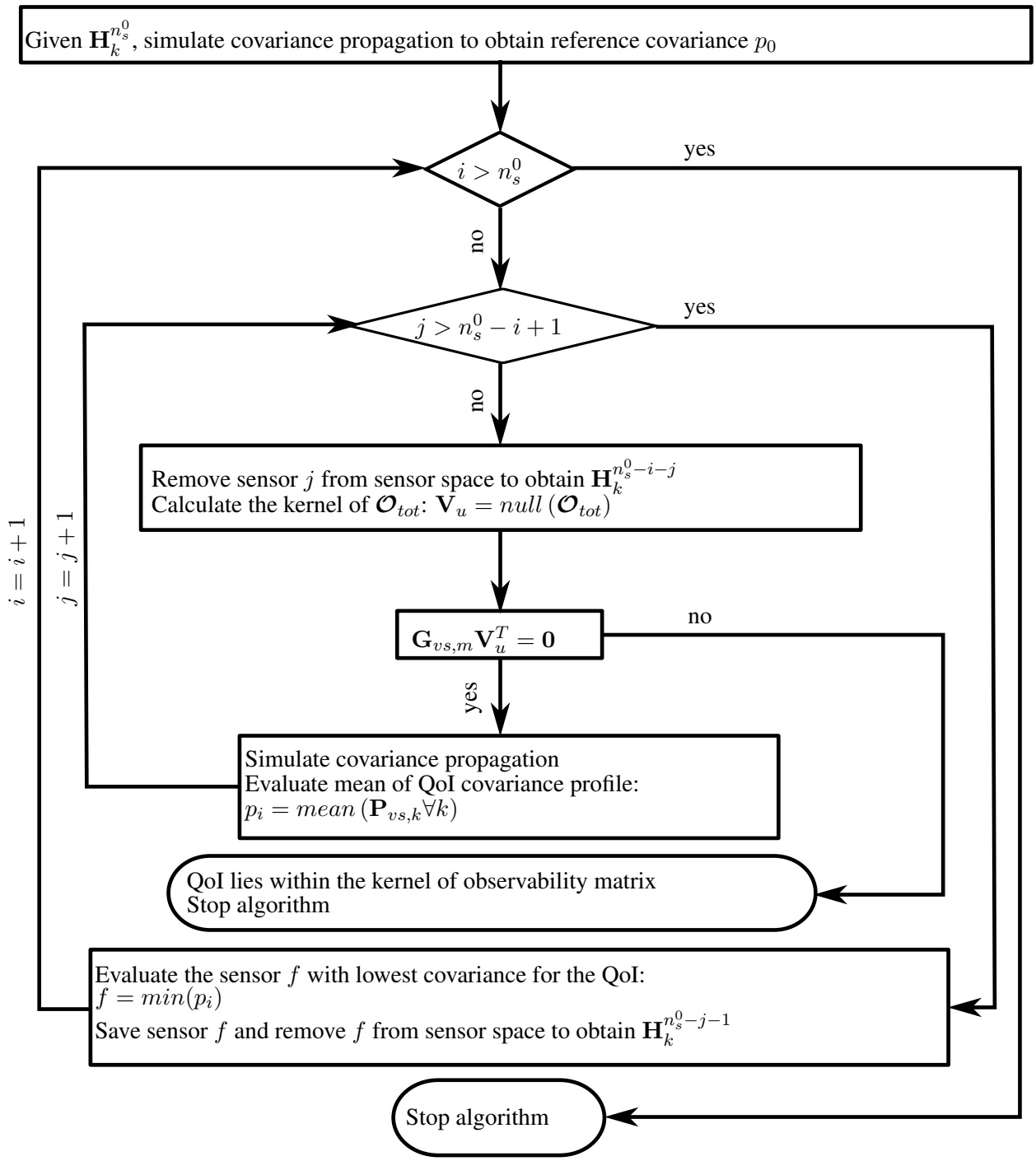


Figure 2: Sensor selection algorithm as presented by Devos et al [3].

Figure 3: The LMSD Concept Car built at the LMSD Research Group at KU Leuven.

1. Evaluate quantity of interest covariance $p_0$ by propagating the covariances $\mathbf{P}_{vs,k}$ for the entire sensor space $\left(\mathbf{H}_k^{n_s^0-i}\right)$
2. Remove sensor $j$ from the sensor space and execute:
   - Calculate total observability matrix kernel: $\mathbf{V}_u = null(\boldsymbol{\mathcal{O}}_{tot})$
   - Check observability criterion from eq. (13)
   - Propagate EKF covariance equations and evaluate the mean of the covariance profile to obtain $p_i$
3. Save the sensor with the lowest covariance rise as this is the worst sensor at this point in the algorithm. Remove this sensor from the sensor space and restart step 2.

During step 2, the observability criterion defined in eq. (13) is checked to ensure that the removed sensor does not lie within the kernel of the total observability matrix. Should this be the case, the estimator will not be able to deliver reliable results on this quantity of interest. This allows the sensor selection methodology to rank the considered sensors according to their relative contribution to the quantity of interest performance while ensuring estimator stability.

## 4 Validation

In this work, the methodology is validated on the LMSD Concept Car platform depicted on figure 3. The LMSD Concept Car is a research platform built at the LMSD Research Group within the Department of Mechanical Engineering at KU Leuven. This validation platform serves as demonstrator for various research activities carried out at the research group.

Firstly, the advanced vehicle model used in the estimator is presented and has been developed in Simcenter Amesim which is a commercial software package. Furthermore, the chosen measurement and quantities of interest are presented. Subsequently, the results of the dynamic coupling analysis are presented and finally, the sensor selection results are shown.

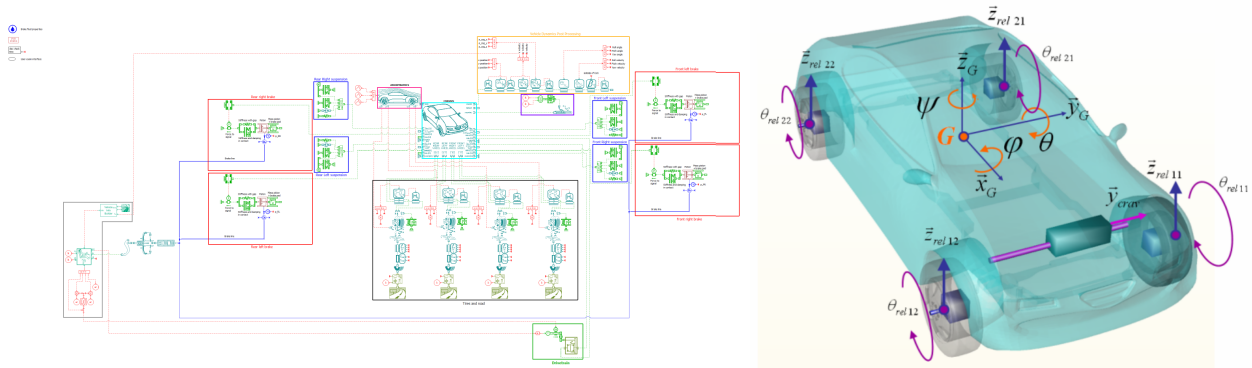


Figure 4: The estimator advanced vehicle model, built in the commercial software package Simcenter Amesim developed by Siemens.

## 4.1 Advanced Vehicle Model

The vehicle model used in this estimator is based on the 15 Degrees Of Freedom (DOF) chassis model with integrated suspension kinematics, steering dynamics and a simple powertrain model containing 77 states in total. This large model is used to show that the sensor selection ranking procedure is able to eliminate more sensors than required for full observability given the independency of the quantities of interest with respect to the unobservable states. This is done because it is likely for models with a high amount of states that the quantities of interest will be independent of some states. This is investigated using dynamic coupling analysis as presented in [9] and is discussed in subsection 4.2.

The following subsections explain the different aspects of the vehicle model, the measurements considered and the quantities of interest.

### 4.1.1 System Model

As mentioned earlier, the vehicle model considered in this work is based on a 15 DOF chassis model with integrated suspension travel, wheel alignment and steering dynamics. Figure 4 shows the vehicle model as implemented in a commercial software package on the left and the corresponding degrees of freedom on the right. Next to the mechanical model, additional features were included such as the brake hydraulics as well as brake piston dynamics. This model contains 77 states in total of which 38 are used for the chassis model including suspension travel and steering dynamics, 3 states are related to the driver model and the others are related to the brake dynamics (24 states for the brake pressures and 12 states for the piston dynamics).

The following paragraphs explain the most important aspects of the vehicle model used in this work:

**Chassis Model** The chassis model consists of a multibody model formulated in state-space format to allow the application of estimation algorithms. The vehicle body is described using the centre of gravity position and velocity and a ZXY Euler angle decomposition with corresponding body rotational velocities.

**Suspension Model** For the suspension, a kinematic relation is used which depends on the vertical travel of the spindle and the road input. Wheel orientation angles are deduced from look-up tables depending on the vertical position of the spindle with respect to the body, the vertical spindle location of the opposite side and the road input.

**Tire Road Interaction** The tire road interaction is modelled using the Magic Formula tire model developped by Pacejka Et Al. [10]. The parameters of the Magic Formula tire model were taken from a standard tire model present in the software. Finally, the assumption was made throughout the entire work that the road is perfectly flat and horizontal.

**Braking System** The braking system is modelled in detail from the brake booster via hydraulic lines to the brake pistons for each wheel. This was done to investigate the influence of brake pressure sensors which were installed on the LMSD Concept Car. It is assumed that each hydraulic line contains 6 pressure nodes which takes into account losses within the hydraulic lines.

**Aerodynamics** Finally, a simple aerodynamic model was used which computes drag, lift and lateral forces depending on the vehicle speed, lateral and vertical wind velocity.

### 4.1.2 Measurement Equations

To be able to make the estimator states fully observable, all relevant measurements have to be taken into account by the sensor selection procedure. Therefore, the measurement vector can be written as:

$$\mathbf{y} = \begin{bmatrix} \mathbf{a}_{cog} & \omega_z & \mathbf{x_{cog}} & \theta_{ij} & \mathbf{p}_{n,ij} & \mathbf{p}_{l,ij} & \mathbf{driver} \end{bmatrix}^T \tag{15}$$

where $\mathbf{a}_{cog}$ represents the acceleration vector in three dimensions, $\omega_z$ the yaw rate, $\mathbf{x_{cog}}$ the position vector of the body center of gravity, $\theta_{ij}$ the rotational speeds of the wheels, $\mathbf{p}_{n,ij}$ the brake pressures for all pressure nodes of the brake hydraulics, $\mathbf{p}_{l,ij}$ the pressure in the brake lines (between the nodes) and $\mathbf{driver}$ are measurements related to the driver control model.

Using eq. (4), the linearized measurement Jacobian $\mathbf{H}_k$ can be deduced and should contain as many rows as elements in the output vector described by eq. (15). As the measurement Jacobian is used in the Kalman filter update step, all sensor equations present in this matrix will be covered by the sensor selection methodology ranking procedure.

### 4.1.3 Quantities of Interest Equations

Next to the measurements, the estimator quantities of interest have to be defined. In this work, the front tire forces and the sideslip angle were chosen as these are commonly estimated using Kalman filter based frameworks ( [11], [12]) such that the quantities of interest vector reads:

$$\mathbf{y}_{vs} = \begin{bmatrix} F_{x,fl} & F_{x,fr} & F_{y,fl} & F_{y,fr} & F_{z,fl} & F_{z,fr} & \beta_{cog} \end{bmatrix}^T \tag{16}$$

Since different quantities of interest might require different sensors for optimal estimation performance, the sensor selection methodology presented in this work can be executed for each of these quantities of interest and could deliver different conclusions per metric.

## 4.2 Dynamic Coupling Analysis

For every estimator, a minimally required sensor set for full observability can be defined which depends on the internal dynamics of the model. In this work, the dynamic coupling analysis method as presented in [9] is used to determine the minimally required sensor set for full observability. Furthermore, the information given by dynamic coupling analysis is used within the sensor ranking procedure until it is no longer possible to stably nor accurately estimate the quantity of interest.

Dynamic coupling analysis makes use of the partitioned, linearized, discrete system Jacobian $\mathbf{F}_{d,k}$ which is depicted on figure 5. From figure 5 it is clear that quite some states are at least partially decoupled which will lead to observability issues when their corresponding sensors are omitted. The figure shows that states 41 to 76 are partially decoupled of which their description is mentioned in table 1. This is because the upper right corner of the system Jacobian is a zero matrix.

Figure 5 shows that states 1 to 32 are fully coupled, states 33 to 40 are coupled to states 1 to 32 but not vice versa, states 41 to 76 are partially decoupled and state 77 is fully decoupled according to the definition presented in figure 1. Since states 1 to 32 are fully coupled, only one sensor is theoretically required to

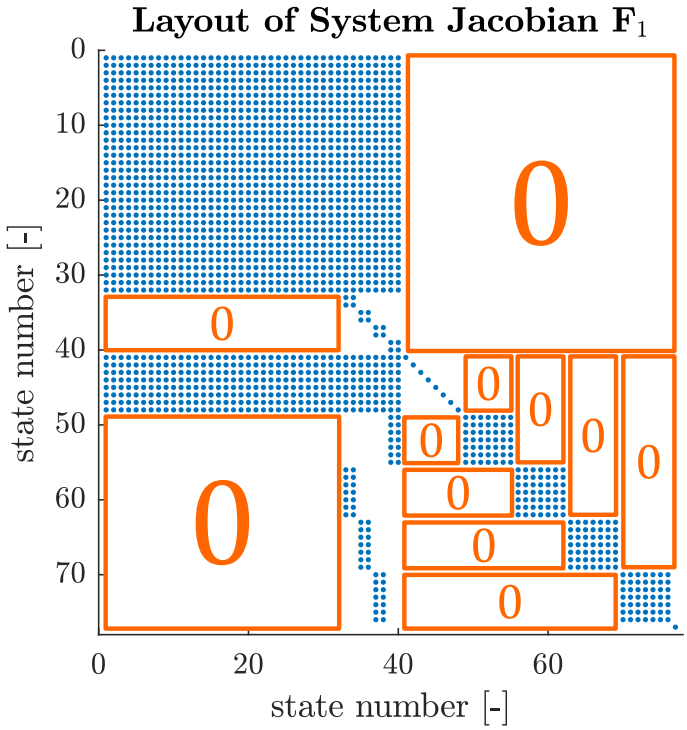


Figure 5: The left figure shows a matrix sparsity pattern of the linearized, discrete system Jacobian required for dynamic coupling analysis. The blue dots indicate that a non-zero value is present.

observe all of these states. However, for each partially or fully decoupled state, an additional sensor would be required to make these states observable except when the partially decoupled states have dependencies towards other decoupled states as indicated by the fully occupied diagonal blocks in figure 5. An example within this vehicle model are states 49 to 76 which represent the brake line pressures for each wheel as they are each represented by 6 nodes. For each of these four blocks, one additional sensor is required for full observability. Therefore, states 41 to 48 and state 77 each require one sensor and for states 49 to 76, four additional sensors would be required for full observability. This leads to a total minimal sensor set of 14 sensors required for full estimator observability.

State 77 is related to the driver model and describes the integration part of the acceleration PID controller. The decoupling analysis shows that this state is fully decoupled from the others and is therefore unnecessary for reliable estimation of the quantities of interest chosen in this work.

Additionally, figure 5 shows that there is only very limited coupling between the brake dynamics and the vehicle dynamics as the brake pressures are only coupled to states 32 to 40. These state represent the brake piston dynamics which in turn depend heavily on the chassis states. From this can be concluded that all states related to brake pressures are only relevant if the quantities of interest have large contributions towards these brake pressure states which is not the case for the chosen quantities of interest in this work.

In conclusion, all three cases presented in figure 1 are present in this larger, more complex model as there are fully coupled states, partially decoupled and fully decoupled states. Decoupling analysis shows that if the brake pressures are not part of the quantities of interest, their contribution to the quantities of interest estimation performance is limited.

## 4.3 Estimator Tuning and Initialization

As this work makes use of an extended Kalman filter, both the measurement noise and process noise matrices $\mathbf{R}$ and $\mathbf{Q}_d$ need to be defined and tuned for optimal results. In this work, this has been done using trial and

Table 1: Decoupled states

| State | Description | State | Description | State | Description |
|---|---|---|---|---|---|
| 41 | Driver 1 | 53 | $p_{n,rl4}$ | 65 | $p_{n,fr2}$ |
| 42 | Driver 2 | 54 | $p_{n,rl5}$ | 66 | $p_{n,fr3}$ |
| 43 | $x_{cog}$ | 55 | $p_{n,rl6}$ | 67 | $p_{n,fr4}$ |
| 44 | $y_{cog}$ | 56 | $p_{l,fl}$ | 68 | $p_{n,fr5}$ |
| 45 | $\theta_{fl}$ | 57 | $p_{n,fl1}$ | 69 | $p_{n,fr6}$ |
| 46 | $\theta_{fr}$ | 58 | $p_{n,fl2}$ | 70 | $p_{l,rr}$ |
| 47 | $\theta_{rl}$ | 59 | $p_{n,fl3}$ | 71 | $p_{n,rr1}$ |
| 48 | $\theta_{rr}$ | 60 | $p_{n,fl4}$ | 72 | $p_{n,rr2}$ |
| 49 | $p_{l,rl}$ | 61 | $p_{n,fl5}$ | 73 | $p_{n,rr3}$ |
| 50 | $p_{n,rl1}$ | 62 | $p_{n,fl6}$ | 74 | $p_{n,rr4}$ |
| 51 | $p_{n,rl2}$ | 63 | $p_{l,fr}$ | 75 | $p_{n,rr5}$ |
| 52 | $p_{n,rl3}$ | 64 | $p_{n,fr1}$ | 76 | $p_{n,rr6}$ |

error which lead to the following noise matrices:

$$\mathbf{R} = \begin{bmatrix} R_{GPS}\mathbf{I}_{2\times2} & & & & & & & & \\ & R_{a_i}\mathbf{I}_{3\times3} & & & & & & & \\ & & R_{gyr} & & & & & & \\ & & & R_{\theta_{ij}}\mathbf{I}_{4\times4} & & & & & \\ & & & & R_{\omega_{ij}}\mathbf{I}_{4\times4} & & & & \\ & & & & & R_{p_{l,ij}}\mathbf{I}_{28\times28} & & & \\ & & & & & & R_{GPS}\mathbf{I}_{2\times2} & & \\ & & & & & & & R_{v_i} \end{bmatrix} \tag{17}$$

where $R_{a_i} = 10^{-3}\ \left(\frac{\text{m}}{\text{s}^2}\right)^2$ is the MEMS accelerometer noise, $R_{gyr} = 10^{-1}\ \left(\frac{\text{m}}{\text{s}}\right)^2$ is the gyroscope noise, $R_{GPS} = 2\ \text{m}^2$ is the GPS noise, $R_{\theta_{ij}} = 10^{-1}\ \text{rad}^2$ is the wheel position encoder noise, $R_{\omega_{ij}} = 10^{-1}\ \left(\frac{\text{rad}}{\text{s}}\right)^2$ is the wheel speed encoder noise, $R_{p_{l,ij}} = 1000\ \text{Pa}^2$ is the pressure sensor noise and $R_{v_i} = 0.5\ \left(\frac{\text{m}}{\text{s}}\right)^2$ is the driver model velocity noise.

Furthermore, the process noise matrix $\mathbf{Q}_d$ was chosen as:

$$\mathbf{Q}_d = 10^{-2}\mathbf{I}_{77\times77} \tag{18}$$

Finally, the extended Kalman filter covariance matrix was initialized to the following values:

$$\mathbf{P}_0 = 10^{-3}\mathbf{I}_{77\times77} \tag{19}$$

## 4.4 Sensor Selection Results and Interpretation

Figure 6 shows the results of the algorithm for the LMDS Concept Car case obtained for each quantity of interest. Therefore, figure 6 contains as many graphs as quantities of interest defined in eq. (16). The resulting graphs in figure 6 shows that different optimal sensor sets can be obtained depending on which quantity of interest is evaluated.

The $x$-axis shows, left to right, the removed sensors from the sensor space during each iteration. Therefore, the left side indicates the entire sensor space and the right side is reached when either no sensors are left or not enough are left to make the quantities of interest observable. Additionally, the blue line indicates the ratio between the covariance $p_i$ for each removed sensor indicated on the $x$-axis and the reference covariance $p_0$ obtained for the entire sensor space:

$$p_{QoI} = \frac{p_i}{p_0} \tag{20}$$

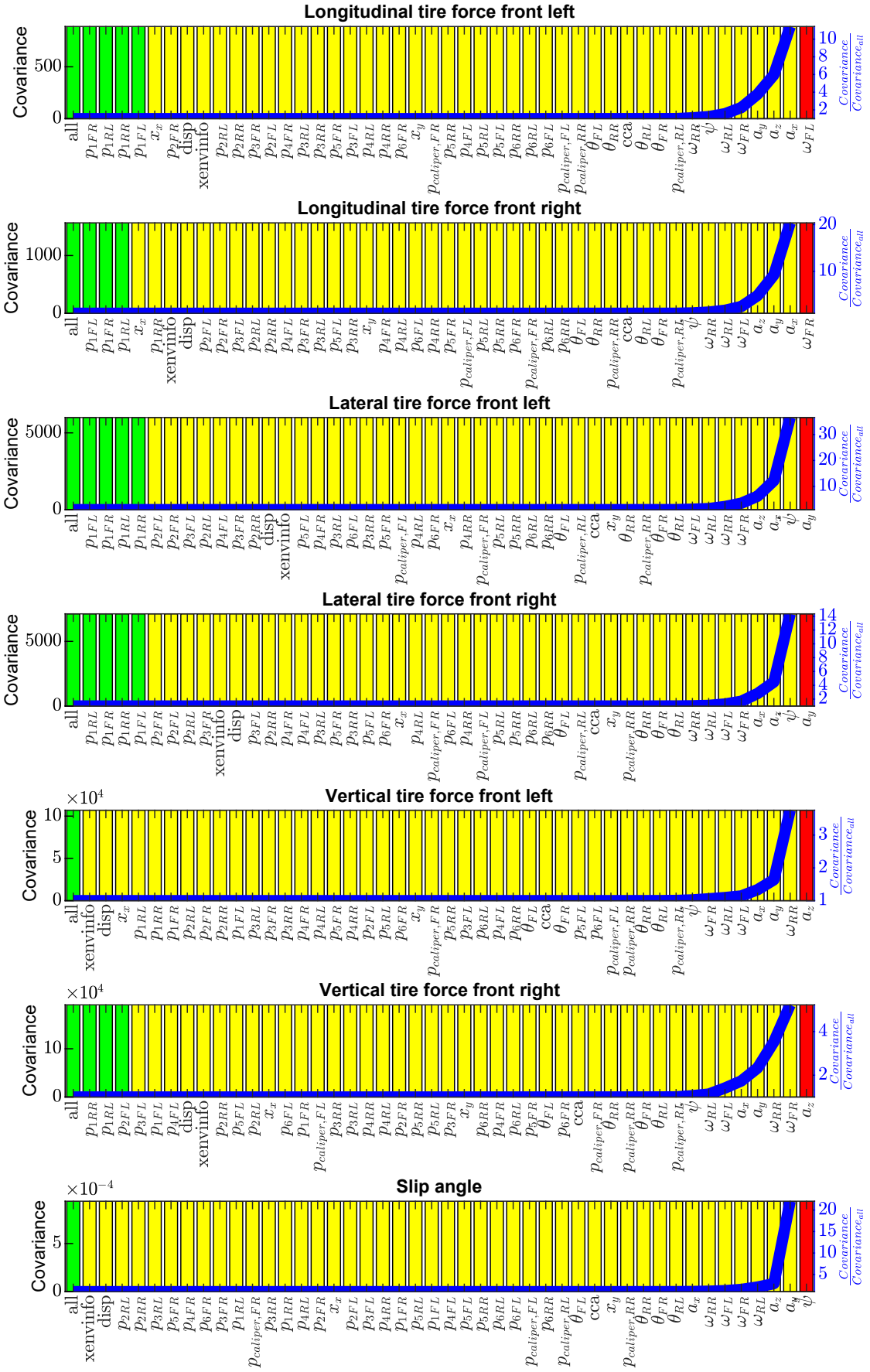


Figure 6: Results of the sensor selection methodology ranking procedure as defined in [3].

which indicates the estimation performance increase obtained by adding the evaluated sensor and is therefore an interesting performance evaluation criterion.

Next to the quantity of interest performance increase, information on observability is also present in the results namely in the bar height and color. The bar height indicates the maximal absolute covariance of the quantity of interest. The bar color indicates whether observability is fulfilled or not. Green means that the estimator is fully observable for the specified sensor set. Yellow means that all states related to the quantities of interest are observable and therefore the estimator unobservable state covariances can be stabilized using the projection defined in eq. (12). Red means that the quantity of interest cannot be estimated reliably with the remaining sensors and therefore sensors have to be added.

For all tire forces, the sensor selection methodology suggests that the accelerations of the center of gravity, the yaw rate and the wheel speeds are the most important sensors. This corresponds to engineering experience as the accelerations are directly linked to the forces in the equations of motion. Additionally, wheel speeds are important to match the vehicle velocity which is required to calculate both the tire longitudinal slip and sideslip angles. An interesting conclusion is that the brake pressures do not contribute significantly to the performance increase of this particular quantity of interest.

A general conclusion could be made that quite some sensors are required to make the estimator fully observable (indicated by the start of the yellow bars), although only a few sensors have significant contributions to the quantities of interest estimation performance (indicated by an exponential rise in the blue line). Using the covariance projection presented in [3], estimators can be stabilized for partially decoupled system dynamics given their independence to the quantities of interest. Therefore, the methodology presented in this work allows state estimators with more complex system models to not necessarily require more sensors simply to make the estimator fully observable, reducing the amount of required sensors for stable operation. Additionally, it is clear from the sensor selection results that, if the brake pressures do not depend on the quantities of interest, they also do not add much value to the estimation performance of the other quantities of interest. Therefore, to save computational effort and memory, the physics of the brake hydraulics could be omitted from the model.

# 5 Conclusions

This work covers the application of a novel sensor selection methodology for partially unobservable, system-level models. The considered sensors are ranked according to their contributions to the quantities of interest estimation performance by evaluating their covariance. Firstly measurements can be obtained either experimentally or virtually by adding white noise to the outputs of a forward simulation. This allows for the sensor selection procedure to be executed before sensors have to be acquired to avoid unnecessary expenses and costly test campaigns.

After the measurement data has been acquired, an extended Kalman filter based estimator is run once for the entire sensor space which allows to save the linearized Jacobians. These Jacobians are used to perform an observability analysis and dynamic coupling analysis. For this vehicle case, a minimal sensor set of 14 sensors is required to make the estimator fully observable. However, there are 26 states dynamically independent which means that they can be stabilized using a projection defined in [3].

Using previously saved Jacobians, the sensor selection algorithm can be run. Each iteration, one sensor is removed from the sensor space after which the estimator covariance equations are evaluated to obtain the new covariance. The sensor which cause the lowest covariance rise is eliminated from the sensor space after which the process is restarted untill either no sensors are left or the quantities of interest are unobservable. The methodology is able to quantitatively indicate the performance increase for each sensor correctly according to engineering experience and is applicable for any type of sensor.

## Acknowledgements

This research was partially supported by Flanders Make, the strategic research centre for the manufacturing industry. The Flanders Innovation & Entrepreneurship Agency within the IMPROVED and MULTISENSOR project is also gratefully acknowledged for its support. Internal Funds KU Leuven are gratefully acknowledged for their support.

## References

[1] R. Cumbo, L. Mazzanti, T. Tamarozzi, P. Jiranek, W. Desmet, and F. Naets, "Advanced optimal sensor placement for kalman-based multiple-input estimation," *Mechanical Systems and Signal Processing*, vol. 160, p. 107830, 2021. [Online]. Available: https://www.sciencedirect.com/science/article/pii/S0888327021002259

[2] R. Semaan, "Optimal sensor placement using machine learning," *Computers & Fluids*, vol. 159, 09 2016.

[3] T. Devos, M. Kirchner, J. Croes, W. Desmet, and F. Naets, "Sensor selection and state estimation for unobservable and non-linear system models," *Sensors*, vol. 21, no. 22, 2021. [Online]. Available: https://www.mdpi.com/1424-8220/21/22/7492

[4] D. Simon, *Optimal State Estimation: Kalman, H Infinity, and Nonlinear Approaches*. USA: John Wiley & Sons, Ltd, 2006. [Online]. Available: https://onlinelibrary.wiley.com/doi/abs/10.1002/0470045345.ch15

[5] K. W. Morton and D. F. Mayers, *Numerical Solution of Partial Differential Equations: An Introduction*, 2nd ed. Cambridge University Press, 2005.

[6] G. Beylkin, J. M. Keiser, and L. Vozovoi, "A new class of time discretization schemes for the solution of nonlinear pdes," *Journal of Computational Physics*, vol. 147, no. 2, pp. 362–387, 1998. [Online]. Available: https://www.sciencedirect.com/science/article/pii/S0021999198960934

[7] A. J. Krener, "The convergence of the extended kalman filter," in *Directions in Mathematical Systems Theory and Optimization*, A. Rantzer and C. I. Byrnes, Eds. Berlin, Heidelberg: Springer Berlin Heidelberg, 2003, pp. 173–182.

[8] S. Banerjee and A. Roy, *Linear Algebra and Matrix Analysis for Statistics (1st ed.)*. USA: Chapman and Hall/CRC, 2014.

[9] T. Devos., M. Kirchner., J. Croes., J. De Smet., and F. Naets., "Design and validation of a multi-objective automotive state estimator for unobservable and non-linear vehicle models," in *Proceedings of the 8th International Conference on Vehicle Technology and Intelligent Transport Systems - VEHITS,*, INSTICC. SciTePress, 2022, pp. 273–280.

[10] E. Bakker, L. Nyborg, and H. B. Pacejka, "Tyre modelling for use in vehicle dynamics studies," *SAE Transactions*, vol. 96, pp. 190–204, 1987. [Online]. Available: http://www.jstor.org/stable/44470677

[11] M. Viehweger, C. Vaseur, S. van Aalst, M. Acosta, E. Regolin, A. Alatorre, W. Desmet, F. Naets, V. Ivanov, A. Ferrara, and A. Victorino, "Vehicle state and tyre force estimation: demonstrations and guidelines," *Vehicle System Dynamics*, vol. 59, no. 5, pp. 675–702, 2021. [Online]. Available: https://doi.org/10.1080/00423114.2020.1714672

[12] B.-C. Chen and F.-C. Hsieh, "Sideslip angle estimation using extended kalman filter," *Vehicle System Dynamics - VEH SYST DYN*, vol. 46, pp. 353–364, 09 2008.